Capillary equilibrium in a semi-solid Al-Cu slurry

Nathalie Limodin, Luc Salvo, Michel Suery, Francis Delannay

Capillary equilibrium in a semi-solid Al–Cu slurry

Nathalie Limodin[a,c], Luc Salvo[a], Michel Suery[a], Francis Delannay[b]
[a] Grenoble INP, SIMAP, Saint-Martin d'Hères Cedex, France
[b] Université catholique de Louvain, Département des Sciences des matériaux et des procédés, Louvain-la-Neuve, Belgium
[c] Present affiliation: INSA de Lyon, MATEIS, Villeurbanne, France

The microstructural evolution of an Al-15.8 wt.% Cu slurry held for 80 min at 555 °C has been characterised in-situ by X-ray microtomography. The different parameters measured by segmentation of the 3D images are analysed by reference to a model describing capillary equilibrium in an aggregate of solid particles with uniform solid/liquid interface curvature. Excellent agreement is found between model predictions and experimental data, except for the fact that the solid/liquid interface area predicted by the model is lower by about 12.5 % than that measured experimentally. This suggests that, owing to the progressive grain coarsening, the slurry does not achieve uniform interface curvature. The model makes possible the conversion of experimental data into evolutions of the dihedral angle, average surface tensions ratio, and capillary pressure in the liquid.

Keywords: Semi-solid processing; Al–Cu alloy; Capillarity; Interface energy; Tomography

1. Introduction

Manufacturing of net shape metallic parts by semi-solid processing is currently arousing intensive development. Optimisation of the casting and/or forming processes requires fine control of the rheology of the metallic slurry, e. g. [1]. In principle, thixotropy is provided by a globular morphology with fine equiaxed solid particles uniformly distributed within the liquid phase. At the temperature of semi-solid forming or casting, the phases constituting the slurry can be considered to be in chemical equilibrium and the evolution of the system is then driven only by capillary forces. In the presence of only two phases, microstructural stability is entirely governed by the relative values of the average solid–liquid and solid–solid interface energies, denoted γ_{sl} and γ_{ss}. A mostly globular microstructure can be obtained only in systems in which γ_{sl} and γ_{ss} are sufficiently isotropic.

A microstructure consisting of solid grains embedded into a continuous liquid phase can be characterised by the following parameters:

- the liquid phase volume fraction

$$u = \frac{V_{\text{liquid}}}{V_{\text{liquid}} + V_{\text{solid}}} \tag{1}$$

- the solid/solid and solid/liquid interface areas per unit volume of the system, a_{ss} and a_{sl};
- the coordination number, n_c, defined as the average number of contacts of each solid grain with other grains;
- the average volume of the particles, V_p.

According to stereology, exact values of u, a_{ss} and a_{sl} can be derived from 2D image analysis. In contrast, the exact values of n_c and V_p are accessible only via 3D characterisation. n_c and V_p can be estimated from 2D images only on the basis of an hypothesis about grain shapes and size distribution [2]. 3D reconstruction of a microstructure can be made by serial sectioning, e. g. [3], but the choicest method for the characterisation of a semi-solid microstructure at the process temperature is fast X-ray microtomography [4, 5]. Indeed, being non-destructive, this method allows in-situ follow-up of the evolution of the local microstructure at high temperature.

If thermodynamic equilibrium with respect to capillary forces prevails in the slurry, the microstructural parameters are related to one another and to the interface energies γ_{sl} and γ_{ss} (which themselves are functions of alloy composition and of the chemical equilibrium between the phases in contact at the interfaces). A model has recently been developed for expressing these relationships in semi-solid systems having reached capillary equilibrium with uniform curvature of the interfaces [6, 7]. This model allows accounting for a larger set of variables than the models currently proposed in the literature for describing the second stage of liquid phase sintering, e. g. [8–11] (during which thermodynamic equilibrium also corresponds to uniform interface curvature). In the present paper, the evolutions of the microstructural parameters measured by in-situ microtomography of an Al–Cu slurry maintained at constant temperature [5] are analysed with reference to this model. The sources of difference between model predictions and experimental data are evaluated. The model is used to derive the evolution, with holding time, of the ratio γ_{sl}/γ_{ss} and of the capillary pressure in the liquid phase.

2. Methods

2.1. Experimental

In Ref. [5], the microstructural evolution of an Al-15.8 wt.% Cu alloy held in the semi-solid state was characterised by fast X-ray microtomography on the ID15 beam line at ESRF Grenoble. Only a summary of the experimental method is given here: the reader is referred to the original reference for details.

The specimen was a cylinder of 1.5 mm diameter and 3 mm height that had been first solidified in a metallic mould in such a way as to obtain a fine equiaxed dendritic starting microstructure which will quickly evolve into a globular microstructure. It was placed on a rotating stage while being held in a small furnace at a temperature of 555 °C (the eutectic temperature of the alloy is 548.2 °C). The recording conditions were such that a final spatial resolution of 2.8 μm was achieved with a scan time smaller than 15 s for a total of 400 projections. A scan was taken every minute from 1 min to 80 min holding. No measurable residual porosity could be detected in the reconstructed 3D objects.

After reconstruction, the images were processed by carrying out successively

(i) a 3D median filtering,
(ii) a 3D segmentation of the solid and liquid phases on the greyscale images,
(iii) after smoothing of the generated surface, a separation of solid particles at each neck following two different methods called hereafter "3D-separation" and "2D-separation" .

The "3D-separation" was carried out on the 3D volume using a built-in Aphelion routine, called "ClusterSplitConvex". This routine automatically computes a 3D distance function, i.e. the minimum distance to the liquid–solid interface, in order to create a basin centred on the solid particle. It then applies a filtering, of which the strength is adjusted to limit the number of basins and to avoid oversegmentation. Finally, it separates the particles using a 3D watershed method. For the "2D-separation" , the reconstructed 3D solid volume was analysed as a stack of 2D slices on which the separation was carried out using the "watershed" routine of the software Image J, which separates touching particles via a 2D watershed method.

From the objects obtained after both 2D- and 3D-separation, the solid/liquid and solid/solid interfaces areas per unit volume of the sample, a_{sl} and a_{ss}, were measured using the relations:

$$a_{sl} = 2 \times N_{sl}$$

$$a_{ss} = 4 \times N_{ss} \quad (2)$$

where N_{sl} and N_{ss} are the number of solid/liquid and solid/solid interfaces intersected per unit length of an arbitrary test line. In the case of the 3D-separated objects, this measurement was done on a stack of 2D slices. The test lines were parallel and regularly spaced with a constant interline- and interslice-spacing of 1 pixel, i.e. 2.8 μm.

2.2. Model

In Ref. [5], 5 microstructural parameters were independently measured by X-ray tomography: the volume fraction of liquid u, the average particle volume V_p, the average particle coordination number n_c, and the solid/liquid and solid/solid interface areas per unit volume a_{sl} and a_{ss}. This set of experimental data thus makes possible the assessment of models involving up to 4 independent variables by comparing any of the measured parameters to the prediction computed using other measured parameters as model variables. In particular, as X-ray tomography provides a precise value for the average coordination n_c, the model should involve n_c as a variable. Unfortunately, models currently available in the sintering literature either are based on a single n_c value (e.g. [9–12]) or assume that n_c is a function of the other variables of the model (e.g. [13]).

In the present work, the analysis is based on a model that was recently developed for predicting the capillary equilibrium in a system consisting of an aggregate of solid particles immersed in a percolating fluid phase in chemical equilibrium with the solid (i.e. temperature and chemical potentials are supposed uniform and the driving force for change results only from interface energies) [6]. The fluid phase may be either a gas or a liquid. At fixed fluid phase volume fraction u and fixed average solid particle volume V_p, the system can reach equilibrium only by accommodation of the particle shapes (which, if the fluid phase is a liquid, develops primarily by diffusion-precipitation) in such a way as to minimise the total capillary energy, F:

$$F = \gamma_{sl} A_{sl} + \gamma_{ss} A_{ss} = \gamma_{sl} \left[A_{sl} + 2 \cos\left(\frac{\psi}{2}\right) A_{ss} \right] \quad (3)$$

where A_{ss} and A_{sl} are the solid/solid and solid/liquid interface areas in the system, ψ is the dihedral angle and γ_{sl} and γ_{ss} are the average solid–liquid and solid–solid interface energies. As represented in Fig. 1, if the system is divided into Voronoï cells embedding each solid particle, the average coordination number n_c of the particles in the system can be taken to be equal to the average number of faces of the cells. The latter thus consists of an assembly of n_c pyramidal prisms, of which the apex is the particle centre of gravity and the basis is one of the cell faces. As illustrated in Fig. 1, the model substitutes these n_c pyramidal prisms by n_c identical cones of revolution, of which the axis is the vector connecting the centres of gravity of the particles in contact. It follows that the angle β at the apex of the cone is related to the average coordination number n_c as [13, 14]:

$$\beta = \arccos\left(1 - \frac{2}{n_c}\right) \quad (4)$$

A particular feature of the model is that n_c does not need to be an integer. In order that interface energy be minimized at thermodynamic equilibrium, the solid–liquid interface developed in the cone sketched in Fig. 1 consists of an axisymmetrical surface of which the average curvature is constant everywhere. The family of surfaces presenting this property is called the Delaunay surfaces and the curves generating these surfaces are called the Delaunay roulettes [15]. Although the problem can be solved exactly, it has been demonstrated that approximating by an arc of circle

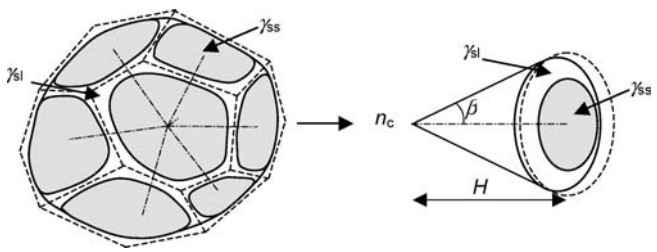

Fig. 1. Representative volume element: the Voronoï cell embedding each solid particle is taken as equivalent to n_c revolution cones of height H and half angle β at the apex.

the curve generating this axisymmetrical surface does not involve a large error in the computation of the minimum energy of the system [7]. The mathematical expressions are given in the literature [6, 7, 16]. These expressions involve 4 independent parameters: u, n_c, V_p, and ψ. Any particular system can thus be described by the model when 4 independent microstructural parameters have been measured. γ_{sl} acts as a scale parameter for the driving forces for change (liquid migration, grain growth, coordination change). It has been shown in Ref. [17] that the predictions of the model agree very well with the predictions of previous models for the intermediate stage of liquid phase sintering that were based on a regular particle packing with integer particle coordination [9–11]. The model has been applied to the investigation of the phenomenon of liquid migration during liquid phase sintering of composition gradient materials [6, 18]. It has also been extended for describing the evolution of the initial stage of sintering of single phase aggregates [17].

3. Results and discussion

As reported in Ref. [5], the liquid volume fraction, u, was observed to progressively stabilise from an initial value $u = 0.34$ towards a plateau at $u = 0.32$ after about 1500 s holding whereas fairly steady state homothetic microstructural coarsening at constant u was observed afterwards. In order to focus only on this steady state microstructural evolution at constant u, we will consider in the following only the parameter evolutions in the interval between 1500 s and 4800 s. The microstructural coarsening during this isothermal holding amounted to an increase of the average particle volume V_p from about 4.9×10^5 μm^3 at $t = 1500$ s to about 6.1×10^5 μm^3 at $t = 4800$ s (as shown later in Fig. 3c). Figure 2 presents the evolution of the average particle coordination number, n_c directly measured on the reconstructed 3D volume (using proper methodology, the evolution of n_c can also be followed by image analysis of 2D sections of the 3D object [19]). It shows that, during microstructural coarsening, the change of the mutual arrangement of contacting grains brings about a decrease in n_c towards an asymptotic value around 6. The change in n_c is slight but, as detailed in Ref. [5], it can be justified by the

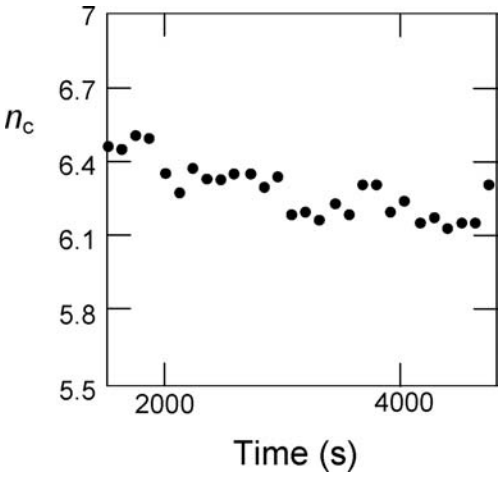

Fig. 2. Evolution of the particle coordination number n_c, with isothermal holding time [5].

observed coarsening mechanism, i.e. a combination of grain coalescence and dissolution–reprecipitation of the smallest grains, which mechanisms affect n_c in opposite ways.

As solid and liquid compositions are constant, a decrease in the free energy F (See Eq. (2)), which drives the evolution of the system, can result from three phenomena: migration of the liquid phase, increase in the average particle size V_p, and change in the average particle coordination number n_c. All three phenomena involve the accommodation of the shape of the solid particles. In particular, computation of the partial derivative of F with respect to n_c for the geometry of the model sketched in Fig. 1 indicates that, at constant u and V_p, the capillary energy decreases if the average coordination n_c decreases [6, 16]. This prediction of the model may justify the decrease in n_c during coarsening shown in Fig. 2 (another possible explanation is proposed below when discussing Fig. 5).

As mentioned in the previous section, the model system is fully determined by 4 parameters whereas X-ray tomography has provided the evolution of 5 microstructural parameters: the volume fraction of liquid u, the average particle volume V_p, the average particle coordination number n_c, and the solid/liquid and solid/solid surface areas per unit volume a_{sl} and a_{ss}. The pertinence of the model for representing the experimental system can thus be assessed by comparing the experimental evolution of any of these 5 parameters to the evolution predicted by the model using the 4 other measured parameters as model parameters for the computations. It is especially enlightening to carry out this exercise for comparing predicted and experimental data for a_{sl}, a_{ss}, and V_p.

Preliminary computations revealed that model and experiments broadly agree. However, some discrepancy was noticed. In particular, experimental values of the solid/liquid interface area a_{sl} were always somewhat larger than the a_{sl} values computed via the model. This discrepancy can be interpreted as due to the fact that the experimental system does not exactly behave like a system at thermodynamic equilibrium, i.e. in which solid/liquid interface curvature is uniform. Although the minimum energy at given V_p and n_c corresponds to uniform curvature, the growth of particles by Ostwald ripening or by grain coalescence cannot occur in the absence of curvature gradients. Indeed, it was shown in Ref. [5] that microstructural coarsening develops by the coalescence of grains, which involves the growth of some necks, the collapse of other necks, and the growth of the biggest grains at the expense of the smallest ones. Hence, the system never reaches a state of uniform curvature, and it can been inferred that capillary energy (which is determined by interface areas through Eq. (2)) always remains higher than the minimum that would be reached in a system with uniform curvature. During the smoothing out of the curvature gradients created by the impingement of two grains, a_{sl} and a_{ss} will tend to decrease and increase, respectively, at rates such that the overall free energy F expressed by (3) decreases. As $a_{sl} > a_{ss}$, we can anticipate that the excess energy with respect to uniform curvature results mainly from an excess of the solid/liquid area a_{sl}.

Of course, the magnitude of the departure between model and experiment cannot be evaluated a priori. Empirically, it was found that the excess of experimental a_{sl} values with

respect to the a_{sl} values computed using the other experimental data as model parameters amounts in average to 12.5 %: the best agreement between model predictions and experimental data was obtained when taking $(a_{sl})_{model} = 0.875\ (a_{sl})_{experiment}$. This is illustrated by the results presented in Fig. 3.

Figure 3a and b presents the evolutions of the surface areas per unit volume a_{sl} and a_{ss}. These graphs reveal that the difference between experimental points obtained using the 2D- or 3D-separation method amounts between 0.5×10^{-3} and 1.0×10^{-3} μm^{-1}. Conspicuously, the two methods very closely agree for the total surface area per unit volume, $a_{sl} + a_{ss}$, but about 15 % larger weight is given to solid/solid interfaces when using the 3D-method than when using the 2D-method. The authors believe that this discrepancy results from the fact that the 2D-method does not accurately enough capture the area of solid–solid necks: for example, necks that are close to parallel to the slicing direction could not be properly detected using the 2D-separation method. The 3D-separation method would thus provide a more accurate estimate of a_{ss}. Nevertheless, all computations mentioned here were carried out using, as input parameters, the average of the a_{sl} and a_{ss} values measured via the two methods.

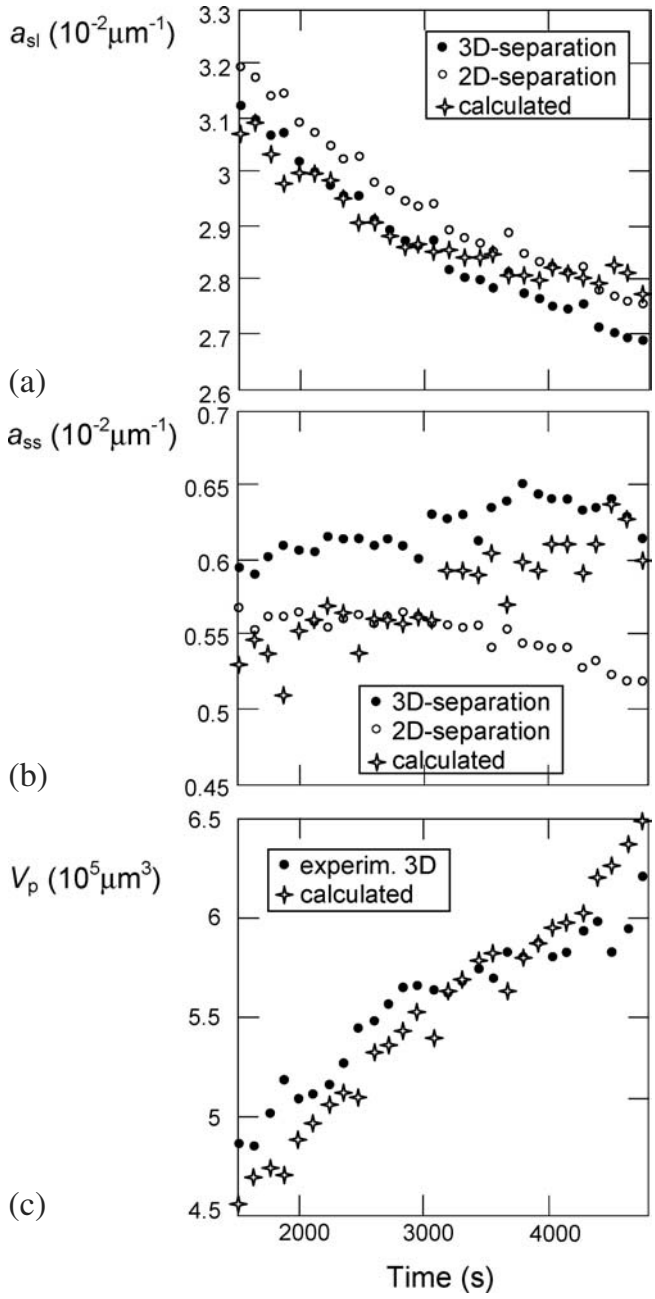

Fig. 3. Comparison of measured microstructural parameters with the parameters calculated by the model. (a) a_{sl}, calculated using the measured values of u, n_c, V_p, and a_{ss}; (b) a_{ss} calculated using the measured values of u, n_c, V_p, and a_{sl}; (c) V_p calculated using the measured values of u, n_c, a_{ss}, and a_{sl}. In each case, the measured a_{sl} values were multiplied by the factor 0.875.

Figure 3a compares the measured a_{sl} values (obtained after 3D- or 2D-separation) multiplied by 0.875 with the a_{sl} values computed via the model using the measured values of u, n_c, V_p, and a_{ss} (taking, for a_{ss}, the average of the values measured after 3D- or 2D-separation). Figure 3b compares the a_{ss} values (measured after 3D- or 2D-separation) with the values predicted by the model using the measured values of u, n_c, and V_p together with $0.875 \times$ the measured a_{sl} (taking the average of the data for 3D- or 2D-separation). Figure 3c compares the measured V_p with the values predicted by the model using the measured values of u, n_c and a_{ss} together with $0.875 \times$ the measured a_{sl} (taking for a_{sl} and a_{ss} the average of the data for 3D- or 2D-separation). All three figures attest to the excellent agreement between computation results and experimental data.

In spite of the fact that, as discussed above, the hypothesis of uniform interface curvature underlying the model does not exactly apply, it is tempting to use the model for deriving microstructural parameters that were not measured by tomography. If capillary equilibrium prevails locally along the triple lines, an essential parameter characterising the system is the dihedral angle ψ. Figure 4 presents an illustration of the particle shapes and necks between particles, as visualised by tomography. Obviously, it would be difficult to evaluate a mean ψ value directly from reconstructed objects such as illustrated in this figure and it can be anticipated that the result would be quite dependent on the resolution of the observation. An alternative is to use the global microstructural parameters measured by tomography for computing, on the basis of the model, a representative value of the ψ angle for the system. The ψ value derived in this way should be less affected by experimental resolution. The computations were carried out using, as input parameters, the same three ensembles of parameters

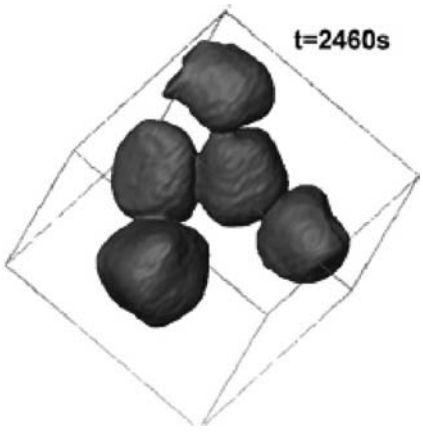

Fig. 4. Illustration of the particle shapes and necks between particles, as visualised by tomography (reproduced from [5], with permission).

used for Fig. 3 (u, n_c, V_p, and a_{ss}; u, n_c, V_p, and a_{sl}; u, n_c, a_{ss}, and a_{sl}) with the measured a_{sl} values multiplied by 0.875. As for Fig. 3, the three different ψ values computed in this way were close. Hence, the data points presented in Fig. 5a are the arithmetic average of these three results. Figure 5a shows that, during holding at 555 °C, ψ increases progressively from 60° to 70°. It is difficult to ascertain whether the results are significantly affected by the departure between the real system and the hypotheses of the model. Although a direct estimation of ψ from the reconstructed volumes is difficult, the range of ψ values on the graph of Fig. 5a does not appear contradicted by the observation of the 3D reconstructed grain presented in Fig. 4. For comparison, according to the graph proposed by German in Fig. 2.30 of Ref. [8], a simple model of interpenetrating spheres predicts, for a system with $\psi = 65°$ and $u = 0.30$, an n_c value close to 4, instead of 6.2 measured experimentally.

Figure 5b presents the values of the ratio $\frac{\gamma_{sl}}{\gamma_{ss}} = \left[2\cos\left(\frac{\psi}{2}\right)\right]^{-1}$ corresponding to Fig. 5a. A low value of γ_{sl}/γ_{ss} is quite expected for a system in which the two phases in equilibrium present a high solubility of the elements in the two phases. The observed range $0.58 \le \gamma_{sl}/\gamma_{ss} \le 0.61$ does not disagree with the range $0.5 < \gamma_{sl}/\gamma_{ss} \cong 0.6$ reported by Camel et al. for the semi-solid systems Zn–Sn, Ag–Pb, Ni–Pb, Al–Sn, and Cu–Pb [20]. This range also agrees with the work of Günduz and Hunt [21] who, for the Al–Cu system at the eutectic temperature, report values of 0.1634 ± 0.021 J m^{-2} for γ_{sl} and 0.3247 ± 0.045 J m^{-2} for γ_{ss} for high angle grain boundaries, i.e. $\gamma_{sl}/\gamma_{ss} \cong 0.503$ with a range $0.38 < \gamma_{sl}/\gamma_{ss} < 0.58$ (taking the estimated errors into account). Figure 5b suggests that the ratio of interface energies γ_{sl}/γ_{ss} increases by about 5 % during microstructural coarsening. If significant, this increase could be ascribed to a progressive decrease in the average solid/solid interface energy γ_{ss}. Indeed, as shown in [5], the coarsening mechanism involves the growth of some of the necks while other necks contract and disappear. As solid/solid interface energies depend on the relative orientation of the contacting grains, it can be anticipated that the necks that disappear have a less favourable orientation than the necks that grow. This phenomenon could also be a possible cause of the progressive decrease in n_c shown in Fig. 2: coordination could progressively tend to $n_c = 6$ in order to favour solid/solid interfaces of type {100}. Justification of this hypothesis would require measurement of the evolution of the average relative orientation of contacting grains during microstructural coarsening.

The partial derivative of F with respect to the volume of liquid, $\left(\frac{\partial F}{\partial V_l}\right)_{n_c,V_p}$, is the "capillary pressure" in the liquid phase, i.e. the pressure difference between the liquid filling the interstices between the particles and the environment outside the sample [6, 9–11] (this pressure difference is called "sphering force" by Park and Yoon [9]). Figure 6 presents the arithmetic averages of the values of the capillary pressure in the liquid (in units of $\gamma_{sl} \times \mu m^{-1}$) calculated by the model using the same three ensembles of input parameters mentioned for Fig. 5. The pressure remains constant and positive (i.e. the liquid tends to be expelled from the system). Its actual magnitude is low: taking $\gamma_{sl} \approx 0.1$ J m^{-2} yields a pressure of about 0.0025 bar, i.e. about $0.25\ \gamma_{sl} V_p^{-1/3}$ (which expresses the fact that $\left(\frac{\partial F}{\partial V_l}\right)_{n_c,V_p}$ scales with the inverse of the particle size). This pressure in the liquid can easily be counterbalanced by the tension carried by the oxide skin which wraps the specimen during holding at 555 °C. This justifies the stability of the slurry during the tomography experiments: in the case of a too high (posi-

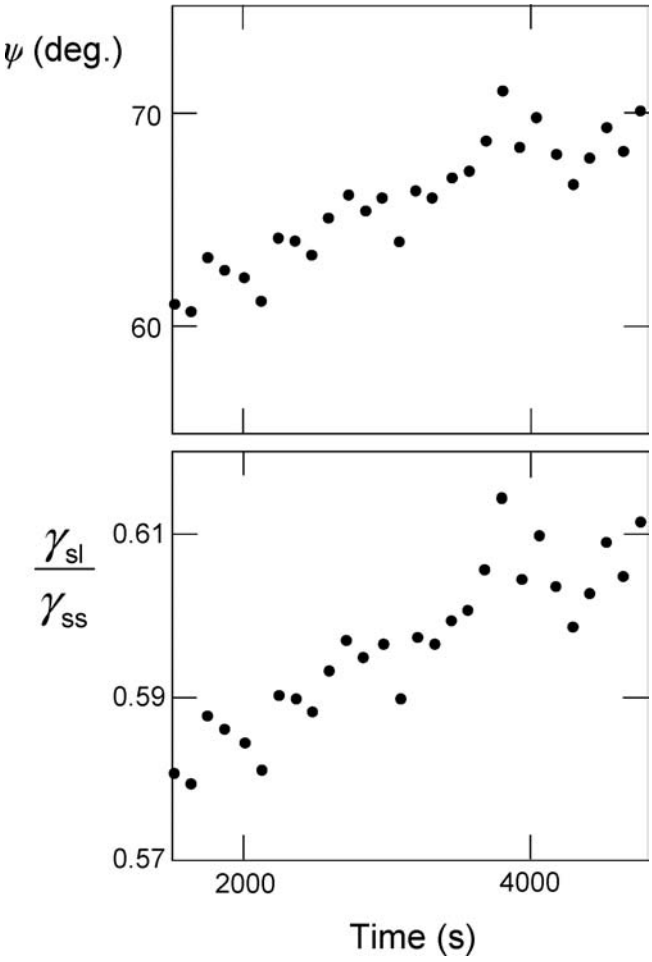

Fig. 5. Arithmetic averages of the values of dihedral angle ψ (a) and ratio γ_{sl}/γ_{ss} (b) calculated by the model using the three ensembles of input parameters mentioned for Fig. 3: u, n_c, V_p, and a_{ss}; u, n_c, V_p, and a_{sl}; u, n_c, a_{ss}, and a_{sl} (with the measured a_{sl} multiplied by 0.875).

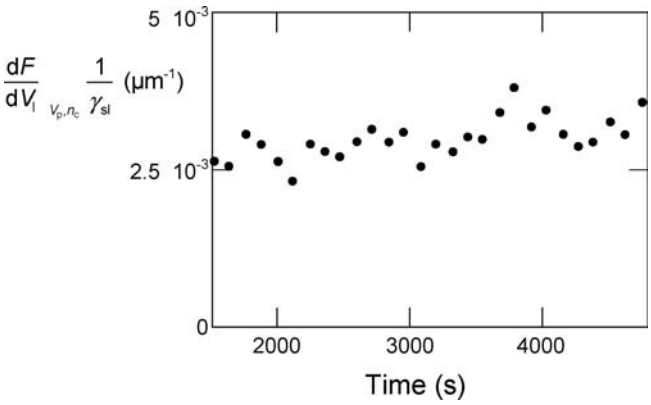

Fig. 6. Arithmetic averages of the values of capillary pressure in the liquid (in units of $\gamma_{sl} \times \mu m^{-1}$) calculated by the model using the same three ensembles of input parameters mentioned for Figs. 3 and 5: u, n_c, V_p, and a_{ss}; u, n_c, V_p, and a_{sl}; u, n_c, a_{ss}, and a_{sl} (with the measured a_{sl} multiplied by the factor 0.875).

tive) capillary pressure, part of the liquid phase would be expelled from the slurry.

4. Conclusions

This work shows the application to a semi-liquid slurry of a model allowing computation of the driving forces for change in a two-phase system with uniform interface curvature in which a fluid phase percolates inside an aggregate of solid particles. The model makes it possible to extract, from microstructural parameters measured by microtomography, intrinsic thermodynamic properties such as the interface energy ratio γ_{sl}/γ_{ss} and the capillary pressure in the liquid. In accordance with model predictions, microstructural coarsening is found to be accompanied by a decrease in the average coordination number n_c. The interface energy ratio increases slightly during holding of the semi-liquid slurry which can be explained by a decrease in the solid–solid interface energy resulting from the gradual disappearance of necks separating particles with less favourable relative orientation.

This work was carried out in the framework of the project ANR-05-BLAN-0286-01 "TOMOSOLIDAL" supported by the "Agence Nationale de la Recherche" which is gratefully acknowledged. F. Delannay gratefully acknowledges the fellowships of INPG-ENSEEG and CNRS supporting his sabbatical period in SIMAP-INPG.

References

[1] M. Suéry: Mise en forme des alliages métalliques à l'état semi-solide, Paris, Editions Lavoisier, 2002.
[2] R.L. Fullman: Trans. AIME 197 (1953) 447–452.
[3] D.J. Rowenhorst, J.P. Kuang, K. Thornton, P.W. Voorhees: Acta Mater. 54 (2006) 2027–2039. DOI:10.1016/j.actamat.2005.12.038
[4] O. Ludwig, M. DiMichiel, P. Falus, L. Salvo, M. Suéry: In Proceedings 8th conference on semi-solid processing of alloys and composites, Limassol, Cyprus, 21–23 September 2004, published as CD-ROM by NADCA, USA.
[5] N. Limodin, L. Salvo, M. Suéry, M. DiMichiel: Acta Mater. 55 (2007) 3177–3191. DOI:10.1016/j.actamat.2007.01.027
[6] F. Delannay, D. Pardoen, C. Colin: Acta Mater. 53 (2005) 1655–1664. DOI:10.1016/j.actamat.2004.12.015
[7] F. Delannay: Philosophical Magazine 85 (2005) 3719–3733. DOI:10.1080/14786430500318860
[8] R.M. German: Liquid phase sintering Plenum Press, New York, 1985.
[9] H.-H. Park, D.N. Yoon: Metall. Trans. A 16A (1985) 923–928.
[10] J. Svoboda, H. Riedel, H. Zipse: Acta Metall. Mater. 42 (1994) 435. DOI:10.1016/0956-7151(94)90498-7
[11] F. Wakai, Y. Shinoda, T. Akatsu: Acta Mater. 52 (2004) 5621. DOI:10.1016/j.actamat.2004.08.021
[12] P.J. Wray: Acta Metall. 24 (1976) 125–135. DOI:10.1016/0001-6160(76)90015-8
[13] R.M. German: Metall. Trans. A 16 (1985) 1247–1252. DOI:10.1007/BF02670329
[14] R.M. German, Z.A. Munir: Metall. Trans. B 6 (1975) 289–94. DOI:10.1007/BF02913572
[15] C.-E. Delaunay: J. Math. Pures et Appl. Sér.1 6 (1841) 309.
[16] F. Delannay, C. Colin: Mater. Sci. Eng. 495 (2008) 236–243. DOI:10.1016/j.msea.2007.09.085
[17] F. Delannay, J.M. Missiaen: Acta Mater. 57 (2009) 420–431. DOI:10.1016/j.actamat.2008.09.019
[18] C. Colin, V. Guipont, F. Delannay: Metall. Mater. Trans. 38A (2007) 150–158. DOI:10.1007/s11661-006-9012-6
[19] N. Limodin, L. Salvo, M. Suéry, F. Delannay: Scripta Materialia 60 (2008) 325–328. DOI:10.1016/j.scriptamat.2008.10.030
[20] D. Camel, N. Eustathopoulos, P. Desré: Acta Metall. 28 (1980) 239. DOI:10.1016/0001-6160(80)90158-3
[21] M. Gündüz, J.D. Hunt: Acta Metall. 33 (1985) 1651–1672. DOI:10.1016/0001-6160(85)90161-0

Correspondence address

Dr. Nathalie Limodin
MATEIS, UMR 5510, INSA de Lyon
69621 Villeurbanne Cedex, France
Tel.: +33 4 72 43 71 76
Fax: +33 4 72 43 85 39
E-mail: nathalie.limodin@gmail.com